

Multicomponent Dark Matter in Radiative Seesaw Model and Monochromatic Neutrino Flux

Mayumi Aoki,^{1,*} Jisuke Kubo,^{1,†} and Hiroshi Takano^{1,2,‡}

¹*Institute for Theoretical Physics, Kanazawa University, Kanazawa 920-1192, Japan*

²*Kavli IPMU (WPI), University of Tokyo, Kashiwa, Chiba 277-8583, Japan*

We consider a two loop radiative seesaw model with an exact $Z_2 \times Z'_2$ symmetry, which can stabilize two or three dark matter particles. The model is a simple extension of the inert scalar model of Ma, where the lepton-number violating mass term of the inert scalar, which is required to be small for small neutrino masses, is generated at the one-loop level. The semi-annihilation processes of different dark matter particles, which are present when there exist more than three different dark matter particles, not only play an important role for their relic densities but also are responsible for the monochromatic neutrino lines resulting from the dark matter annihilation processes. The monochromatic neutrinos do not suffer from a chiral suppression, and we investigate the observational possibility of the monochromatic neutrino flux from the Sun.

PACS numbers: 95.35.+d, 95.85.Pw, 11.30.Er, 14.60.Pq

arXiv:1408.1853v2 [hep-ph] 10 Nov 2014

* mayumi@hep.s.kanazawa-u.ac.jp

† jik@hep.s.kanazawa-u.ac.jp

‡ hiroshi.takano@ipmu.jp

I. INTRODUCTION

Tiny neutrino masses and the absence of dark matter (DM) candidates are problems of the standard model (SM), which can be overcome only by its extension. The tiny neutrino masses can be explained by the seesaw mechanism [1], which usually requires an introduction of right-handed neutrinos with lepton-number violating Majorana masses. However, for the tree-level seesaw mechanism to work, an undesirable hierarchy in the mass scale or in the size of the Yukawa couplings has to be introduced: To obtain neutrino masses of $\mathcal{O}(0.1)$ eV in the type I seesaw for instance, we need either large Majorana masses of Grand Unified Theory scale or very small Yukawa couplings of $\mathcal{O}(10^{-6})$ of the right-handed neutrinos with the left-handed ones if the Majorana masses are $\mathcal{O}(1)$ TeV. This unwelcome feature can be avoided if the neutrino masses are generated radiatively ([2]-[3] for instance). With an increasing number of loops, the hierarchy between the SM scale and the Majorana masses becomes milder, and in fact the Majorana masses can become $\mathcal{O}(1)$ TeV without making the Yukawa couplings very small. The common feature of the radiative seesaw models is the existence of an unbroken discrete symmetry, which forbids the appearance of Dirac neutrino masses. An important consequence of this unbroken symmetry, usually Z_2 , is that the lightest Z_2 odd particle is stable and hence can be a DM candidate with a mass of $\mathcal{O}(1)$ TeV.

In the one-loop radiative seesaw model of Ma [3], the lepton-number violating mass term of the inert doublet scalar η is required to be very small to obtain small neutrino masses. The mass term originates from a lepton-number violating quartic scalar coupling, the " λ_5 coupling", which is $\mathcal{O}(10^{-5})$ to obtain small neutrino masses with the Yukawa couplings of $\mathcal{O}(0.01)$. In this paper, we consider an extension of the model such that this lepton-number violating mass, too, is generated radiatively. Consequently, the seesaw mechanism occurs at the two-loop level in the extended model [4] (A similar idea has been proposed in an E_6 inspired model [5].). For this mechanism to work, we have to introduce a larger unbroken discrete symmetry, $Z_2 \times Z_2$, which implies that the model yields a multicomponent DM system [5]-[10]. We emphasize that the multicomponent DM system is a consequence of the unbroken $Z_2 \times Z_2$, which forbids the Dirac neutrino masses and also the one-loop neutrino mass diagram.

In [4] we have investigated in the extended model the two-component DM system consisting of a neutral component of η and another real scalar χ . We have found that the χ DM can cover the shortage of the relic density of the η DM for the mass range $100 \text{ GeV} \lesssim m_\eta \lesssim 600 \text{ GeV}$ [11, 12]. We were motivated by the desire to explain at the same time a slight excess of the Higgs decay into two γ 's [13] and the 135 GeV γ -ray line possibly observed at the Fermi LAT [14] by the annihilation of the χ DM. Though it is not impossible to explain both γ excesses, we have to use a corner of the parameter space, which faces the border of perturbation theory. Moreover, the subsequent experimental searches could not confirm these interesting γ excesses [15, 16].

In this paper we consider the same model in the parameter space leading to a three-component DM system: Our DM candidates are the lightest right-handed neutrino N , and two real scalars ϕ_R and χ . The semi-annihilation processes of these DM particles have a considerable influence on their relic densities [7, 10], and the monochromatic neutrino lines can be produced from the semi-annihilation process such as $\phi_R \chi \rightarrow N \nu$. These monochromatic neutrinos are not chirally suppressed, and we analyze the observational prospect of the monochromatic neutrino flux from the Sun. Semi-annihilations of DM particles can produce line spectra of neutral SM particles, e.g.

TABLE I. The matter contents of the model and the corresponding quantum numbers. $Z_2 \times Z'_2$ is the unbroken discrete symmetry, while the lepton number L is softly broken by the ϕ mass.

| field | statistics | $SU(2)_L$ | $U(1)_Y$ | Z_2 | Z'_2 | L |
|---------------------------|------------|-----------|----------|-------|--------|-----|
| (ν_L, l_L) | F | 2 | $-1/2$ | + | + | 1 |
| l_R^c | F | 1 | 1 | + | + | -1 |
| N_R^c | F | 1 | 0 | - | + | 0 |
| $H = (H^+, H^0)$ | B | 2 | $1/2$ | + | + | 0 |
| $\eta = (\eta^+, \eta^0)$ | B | 2 | $1/2$ | - | + | -1 |
| χ | B | 1 | 0 | + | - | 0 |
| ϕ | B | 1 | 0 | - | - | 1 |

neutrinos [10] and photons [8], and observations of such line spectra are indications of a multicomponent DM Universe ¹.

II. MODEL

Here we will briefly outline the model [4], where we show the matter content of the model in Table I. In addition to the matter content of the SM model, we introduce the right-handed neutrino N_R^c , an $SU(2)_L$ doublet scalar η , and two SM singlet scalars χ and ϕ . Note that the lepton number L of N_R^c is zero. The $Z_2 \times Z'_2 \times L$ -invariant Yukawa sector and Majorana mass term for N_R^c can be described by

$$\mathcal{L}_Y = Y_{ij}^e H^\dagger L_i l_{Rj}^c + Y_{ik}^\nu L_i \epsilon \eta N_{Rk}^c - \frac{1}{2} M_k N_{Rk}^c N_{Rk}^c + h.c. , \quad (1)$$

where i, j, k ($= 1, 2, 3$) stand for the flavor indices. The scalar potential V is written as $V = V_\lambda + V_m$, where

$$\begin{aligned} V_\lambda = & \lambda_1 (H^\dagger H)^2 + \lambda_2 (\eta^\dagger \eta)^2 + \lambda_3 (H^\dagger H)(\eta^\dagger \eta) + \lambda_4 (H^\dagger \eta)(\eta^\dagger H) \\ & + \gamma_1 \chi^4 + \gamma_2 (H^\dagger H) \chi^2 + \gamma_3 (\eta^\dagger \eta) \chi^2 + \gamma_4 |\phi|^4 + \gamma_5 (H^\dagger H) |\phi|^2 \\ & + \gamma_6 (\eta^\dagger \eta) |\phi|^2 + \gamma_7 \chi^2 |\phi|^2 + \frac{\kappa}{2} [(H^\dagger \eta) \chi \phi + h.c.] , \end{aligned} \quad (2)$$

$$V_m = m_1^2 H^\dagger H + m_2^2 \eta^\dagger \eta + \frac{1}{2} m_3^2 \chi^2 + m_4^2 |\phi|^2 + \frac{1}{2} m_5^2 [\phi^2 + (\phi^*)^2] . \quad (3)$$

The potential V , except the last term in V_m , is $Z_2 \times Z'_2 \times L$ -invariant. This last term breaks the lepton number softly. In the absence of this term, there will be no neutrino mass. Note that the “ λ_5 term”, $(1/2)\lambda_5(H^\dagger \eta)^2$, is also forbidden by L . A small λ_5 of the original model of Ma [3] is “natural” according to ‘t Hooft [18], because the absence of λ_5 implies an enhancement of symmetry. In fact, if λ_5 is small at some scale, it remains small for other scales as one can explicitly verify [19]. Here we attempt to derive the smallness of λ_5 dynamically, such that the λ_5 term becomes calculable.

¹ Semi-annihilation processes exist also in one-component DM systems when DM is a Z_3 charged particle [7] or a vector boson [17].

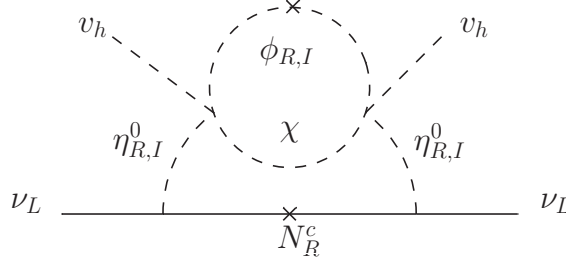


FIG. 1. The two-loop diagram that is responsible for the radiative generation of the neutrino mass. The one-loop self-energy diagram inside of this two-loop diagram is the origin of the mass difference between $m_{\eta_R^0}$ and $m_{\eta_I^0}$ as well as the effective coupling λ_5^{eff} in Eq. (9).

The charged, CP even and odd scalars are defined as

$$H = \begin{pmatrix} H^+ \\ (v_h + h + iG)/\sqrt{2} \end{pmatrix}, \quad \eta = \begin{pmatrix} \eta^+ \\ (\eta_R^0 + i\eta_I^0)/\sqrt{2} \end{pmatrix}, \quad \phi = (\phi_R + i\phi_I)/\sqrt{2}, \quad (4)$$

where v_h is the vacuum expectation value. The tree-level masses of the scalars are given by

$$m_h^2 = 2\lambda_1 v_h^2, \quad (5)$$

$$m_{\eta^\pm}^2 = m_2^2 + \frac{1}{2}\lambda_3 v_h^2, \quad m_{\eta_R^0}^2 = m_{\eta_I^0}^2 = m_2^2 + \frac{1}{2}(\lambda_3 + \lambda_4)v_h^2, \quad (6)$$

$$m_{\phi_R}^2 = m_4^2 + m_5^2 + \gamma_5 v_h^2, \quad m_{\phi_I}^2 = m_4^2 - m_5^2 + \gamma_5 v_h^2, \quad (7)$$

$$m_\chi^2 = m_3^2 + \gamma_2 v_h^2. \quad (8)$$

As we see from (6), the tree-level mass of η_R^0 is the same as that of η_I^0 . At the one-loop level, this degeneracy is lifted because the λ_5 term is generated at this order:

$$\begin{aligned} \lambda_5^{\text{eff}} &= -\frac{\kappa^2}{64\pi^2} \left[\frac{m_{\phi_I}^2}{m_{\phi_I}^2 - m_\chi^2} \ln \frac{m_{\phi_I}^2}{m_\chi^2} - \frac{m_{\phi_R}^2}{m_{\phi_R}^2 - m_\chi^2} \ln \frac{m_{\phi_R}^2}{m_\chi^2} \right] \\ &\sim -\frac{\kappa^2}{64\pi^2} \frac{m_5^2}{m_{\phi_R}^2 - m_\chi^2} \left[1 - \frac{m_\chi^2}{m_{\phi_R}^2 - m_\chi^2} \ln \frac{m_{\phi_R}^2}{m_\chi^2} \right] \text{ for } m_5 \ll m_{\phi_R}. \end{aligned} \quad (9)$$

In other words the origin of this correction is the one-loop self-energy diagram that can be embedded into the two-loop diagram to generate the neutrino mass (see Fig. 1):

$$\begin{aligned} (\mathcal{M}_\nu)_{ij} &= \frac{Y_{ik}^\nu Y_{jk}^\nu}{16(4\pi)^4} \kappa^2 v_h^2 M_k (m_{\phi_I}^2 - m_{\phi_R}^2) \int_0^1 dx_1 \int_0^{1-x_1} dx_2 \int_0^1 dy \left(\frac{y}{\beta - (x_1 - x_1^2)M_k^2} \right) \\ &\times \left[\frac{x_1 - x_1^2}{(1-y)\beta + y(x_1 - x_1^2)m_{\eta^0}^2} - \frac{1}{(1-y)M_k^2 + ym_{\eta^0}^2} \right], \end{aligned} \quad (10)$$

where $\beta \equiv m_{\phi_I}^2 + x_1(m_\chi^2 - m_{\phi_R}^2) + x_2(m_{\phi_I}^2 - m_{\phi_R}^2)$, and we have assumed that $m_{\eta^0} = m_{\eta_R^0} \simeq m_{\eta_I^0}$. Using λ_5^{eff} given in (9), the neutrino mass matrix can be approximated as

$$(\mathcal{M}_\nu)_{ij} = -\frac{\lambda_5^{\text{eff}} v_h^2}{8\pi^2} \sum_k \frac{Y_{ik}^\nu Y_{jk}^\nu M_k}{m_{\eta^0}^2 - M_k^2} \left[1 - \frac{M_k^2}{m_{\eta^0}^2 - M_k^2} \ln \frac{m_{\eta^0}^2}{M_k^2} \right]. \quad (11)$$

We see from (10) that the neutrino mass matrix \mathcal{M}_ν is proportional to $|Y^\nu \kappa|^2 m_5^2$ (because $(m_{\phi_R}^2 - m_{\phi_I}^2) = 2m_5^2$). Therefore, only this combination for a given set of m_χ , m_{ϕ_R} , m_{η^0} and M_k can be fixed by the neutrino mass:

$m_\chi, m_{\phi_R}, m_{\eta^0}, M_k \sim \mathcal{O}(10^2)$ GeV, for instance, implies that $|Y^\nu \kappa| m_5 \sim \mathcal{O}(10^{-2})$ GeV to obtain the neutrino mass scale of $\mathcal{O}(0.1)$ eV. With the same set of the parameter values we find that $\lambda_5^{\text{eff}} \sim 10^{-4}$, where the smallness λ_5^{eff} is a consequence of the radiative generation of this coupling. As we will see, the product $|Y^\nu \kappa|$ enters into the semi-annihilation of DM particles that produces monochromatic neutrinos, while the upper bound of $|Y^\nu|$ follows from the $\mu \rightarrow e\gamma$ constraint.

A. The stability of the scalar potential and the perturbativity constraint

If the parameters of the scalar potential $V = V_\lambda + V_m$ satisfy the following conditions, the potential is bounded from below and the DM stabilizing symmetry $Z_2 \times Z'_2$ remains unbroken at the tree-level:

$$\begin{aligned}
& m_1^2 < 0, \quad m_2^2 > 0, \quad m_3^2 > 0, \quad m_4^2 > 0, \quad |m_5^2| < m_4^2, \\
& \lambda_1 > 0, \quad \lambda_2 > 0, \quad \gamma_1 > 0, \quad \gamma_4 > 0, \\
& \lambda_3 > -\frac{2}{3}\sqrt{\lambda_1 \lambda_2}, \quad \lambda_3 + \lambda_4 > -\frac{2}{3}\sqrt{\lambda_1 \lambda_2}, \\
& \gamma_2 > -\frac{2}{3}\sqrt{\lambda_1 \gamma_1}, \quad \gamma_3 > -\frac{2}{3}\sqrt{\lambda_2 \gamma_1}, \quad \gamma_5 > -\frac{2}{3}\sqrt{\lambda_1 \gamma_4}, \\
& \gamma_6 > -\frac{2}{3}\sqrt{\lambda_2 \gamma_4}, \quad \gamma_7 > -\frac{2}{3}\sqrt{\gamma_1 \gamma_4}, \\
& |\kappa| < \lambda_1 + \lambda_2 + \gamma_1 + \gamma_4 - \frac{2}{3} \left(\sqrt{\lambda_1 \lambda_2} + \sqrt{\lambda_1 \gamma_1} + \sqrt{\lambda_1 \gamma_4} + \sqrt{\lambda_2 \gamma_1} + \sqrt{\lambda_2 \gamma_4} + \sqrt{\gamma_1 \gamma_4} \right).
\end{aligned} \tag{12}$$

We further assume that $|\lambda_i|, |\gamma_i|, |\kappa| < 1$ ensures the perturbativeness of the model. Under these assumptions, it is noted that the above stability conditions give $|\kappa| \lesssim 0.4$.

B. $\mu \rightarrow e\gamma$ constraint

The strongest constraint on Y^ν comes from $\mu \rightarrow e\gamma$ ², which is given by [21, 22]

$$\begin{aligned}
B(\mu \rightarrow e\gamma) &= \frac{3\alpha}{64\pi(G_F m_{\eta^\pm}^2)^2} \left| \sum_k Y_{\mu k}^\nu Y_{ek}^\nu F_2 \left(\frac{M_k^2}{m_{\eta^\pm}^2} \right) \right|^2 \lesssim 5.7 \times 10^{-13}, \\
F_2(x) &= \frac{1}{6(1-x)^4} (1 - 6x + 3x^2 + 2x^3 - 6x^2 \ln x).
\end{aligned} \tag{13}$$

A similar, but slightly weaker bound for $\tau \rightarrow \mu(e)\gamma$ given in [23] has to be satisfied, too. Since $F_2(x) \sim 1/3x$ for $x \gg 1$, while $1/12 < F_2(x) < 1/6$ for $0 < x < 1$, the constraint can be readily satisfied if $M_k \gg m_{\eta^\pm}$ or $M_k < m_{\eta^\pm}$. If we assume that $M_k \sim m_{\eta^\pm} \sim \mathcal{O}(10^2)$ GeV in (13), the constraint (13) becomes $B(\mu \rightarrow e\gamma) \simeq 10^{-4} \times |\sum_k Y_{\mu k}^\nu Y_{ek}^\nu|^2 \lesssim 5.7 \times 10^{-13}$. Therefore, $|Y_{ek}^\nu Y_{\mu k}^\nu|^2 \lesssim \mathcal{O}(10^{-8})$ can satisfy the constraint.

² The more detailed analysis of the lepton flavor violation such as the three body decays of lepton in the Ma model is discussed in Ref.[20].

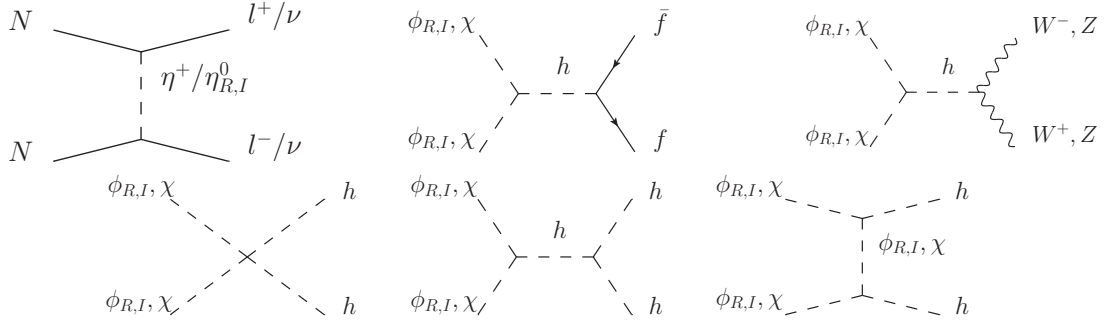


FIG. 2. The diagrams for the standard annihilation processes.

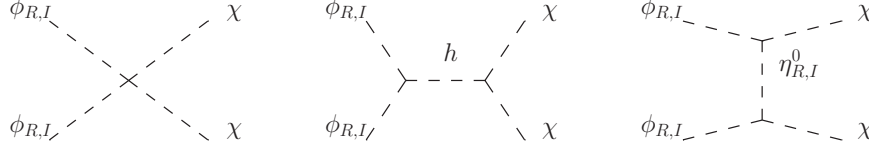


FIG. 3. The diagrams for the DM conversion processes.

C. The T parameter constraint

Of the S, T and U parameters from the electroweak precision measurements the T parameter constraint is the severest for the present model [11, 24, 25],

$$\Delta T \simeq 1.08 \left(\frac{m_{\eta^\pm} - m_{\eta_R^0}}{v_h} \right) \left(\frac{m_{\eta^\pm} - m_{\eta_I^0}}{v_h} \right) = 0.10 \pm 0.08 \quad (14)$$

for $m_h = 125.6 \pm 0.3$ GeV. Therefore, $|m_{\eta^\pm} - m_{\eta_R^0}|$, $|m_{\eta^\pm} - m_{\eta_I^0}| \lesssim 90$ GeV is sufficient to meet the requirement.

III. MULTICOMPONENT DARK MATTER SYSTEM

In this model there are three types of dark matter candidates $N = N_{R1}^c$ (the lightest among N_{Rk}^c 's) or η_R^0 (or η_I^0) with $(Z_2, Z_2') = (-, +)$, χ with $(Z_2, Z_2') = (+, -)$ and ϕ_R (or ϕ_I) with $(Z_2, Z_2') = (-, -)$. For $(Z_2, Z_2') = (-, +)$ there are two candidates, and in the following discussions we assume that N is a DM candidate³. Therefore, our system consists of three DM particles, N , ϕ_R , χ . Consequently, there are three types of DM annihilation

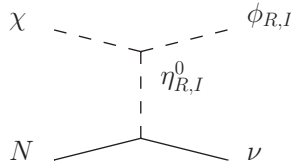


FIG. 4. The diagrams for the semi-annihilation process.

³ The other possibility, η_R^0 -DM, is discussed in [4].

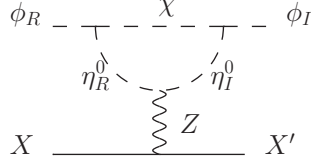


FIG. 5. Conversion process between ϕ_I and ϕ_R . Here X and X' are SM particles.

process [10] (Figures 2-4);

$$\text{Standard annihilation : } NN \rightarrow XX', \quad \phi_R\phi_R \rightarrow XX', \quad \chi\chi \rightarrow XX', \quad (X, X': \text{SM particles}), \quad (15)$$

$$\text{DM conversion : } \phi_R\phi_R \rightarrow \chi\chi, \quad (16)$$

$$\text{Semi-annihilation : } N\phi_R \rightarrow \chi\nu, \quad \chi N \rightarrow \phi_R\nu, \quad \phi_R\chi \rightarrow N\nu, \quad (17)$$

where we assume $m_{\phi_R} > m_\chi$. Moreover, since the mass difference between ϕ_R and ϕ_I is controlled by the lepton-number breaking mass m_5 , which is assumed to be much smaller than m_{ϕ_R} so that m_{ϕ_R} and m_{ϕ_I} are practically degenerate, the contribution of ϕ_I to the annihilation processes during the decoupling of DMs is non-negligible. The annihilation processes of ϕ_I are $\phi_I\phi_I \rightarrow XX'$ (standard annihilation), $\phi_I\phi_I \rightarrow \phi_R\phi_R$ and $\phi_I\phi_I \rightarrow \chi\chi$ (DM conversion), $N\phi_I \rightarrow \chi\nu$, $\chi N \rightarrow \phi_I\nu$ and $\phi_I\chi \rightarrow N\nu$ (semi-annihilation), where we have assumed that the decay of $\phi_I \rightarrow N\chi$ is kinematically forbidden. There is a conversion between ϕ_R and ϕ_I , and its main process is shown in Fig. 5. This process is loop suppressed, and the cross section

$$\sigma_{\phi_I X \rightarrow \phi_R X'} |v| \sim 10^{-14} \times \left(\frac{v_h}{246 \text{ GeV}} \right)^4 \left(\frac{m_\phi}{100 \text{ GeV}} \right)^2 \left(\frac{(100 \text{ GeV})^6}{m_{\eta_R}^2 m_{\eta_I}^2 m_\chi^2} \right) \text{ GeV}^{-2} \quad (18)$$

would be roughly 2 orders of magnitude smaller than that of tree-level processes. The reaction rate of this process is $\langle \sigma_{\phi_I X \rightarrow \phi_R X'} |v| \rangle n_{\phi_I} n_X$ which is roughly $n_{\phi_I}^{-1} \sim \exp(m_{\phi_I}/T)$ times larger than the standard annihilation. Thus, during the decoupling of DMs, the reaction between ϕ_I and ϕ_R can reach chemical equilibrium, implying that we can use a similar method as [26] and sum up the number densities of particles having the same $Z_2 \times Z'_2$ parities. The Boltzmann equations of their number densities n_N , $n_\phi \equiv n_{\phi_I} + n_{\phi_R}$, n_χ are given by

$$\begin{aligned} \dot{n}_N + 3Hn_N = & - \left\{ \langle \sigma_{NN \rightarrow XX'} |v| \rangle (n_N^2 - \bar{n}_N^2) \right. \\ & + \langle \sigma_{N\phi \rightarrow \chi\nu} |v| \rangle (n_N n_\phi - \bar{n}_N \bar{n}_\phi \frac{n_\chi}{\bar{n}_\chi}) + \langle \sigma_{N\chi \rightarrow \phi\nu} |v| \rangle (n_N n_\chi - \bar{n}_N \bar{n}_\chi \frac{n_\phi}{\bar{n}_\phi}) \\ & \left. - \langle \sigma_{\phi\chi \rightarrow N\nu} |v| \rangle (n_\phi n_\chi - \bar{n}_\phi \bar{n}_\chi \frac{n_N}{\bar{n}_N}) \right\}, \end{aligned} \quad (19)$$

$$\begin{aligned} \dot{n}_\phi + 3Hn_\phi = & - \left\{ \langle \sigma_{\phi\phi \rightarrow XX'} |v| \rangle (n_\phi^2 - \bar{n}_\phi^2) + \langle \sigma_{\phi\phi \rightarrow \chi\chi} |v| \rangle (n_\phi^2 - \bar{n}_\phi^2 \frac{n_\chi^2}{\bar{n}_\chi^2}) \right. \\ & + \langle \sigma_{N\phi \rightarrow \chi\nu} |v| \rangle (n_N n_\phi - \bar{n}_N \bar{n}_\phi \frac{n_\chi}{\bar{n}_\chi}) - \langle \sigma_{N\chi \rightarrow \phi\nu} |v| \rangle (n_N n_\chi - \bar{n}_N \bar{n}_\chi \frac{n_\phi}{\bar{n}_\phi}) \\ & \left. + \langle \sigma_{\phi\chi \rightarrow N\nu} |v| \rangle (n_\phi n_\chi - \bar{n}_\phi \bar{n}_\chi \frac{n_N}{\bar{n}_N}) \right\}, \end{aligned} \quad (20)$$

$$\begin{aligned} \dot{n}_\chi + 3Hn_\chi = & - \left\{ \langle \sigma_{\chi\chi \rightarrow XX'} |v| \rangle (n_\chi^2 - \bar{n}_\chi^2) - \langle \sigma_{\phi\phi \rightarrow \chi\chi} |v| \rangle (n_\phi^2 - \bar{n}_\phi^2 \frac{n_\chi^2}{\bar{n}_\chi^2}) \right. \\ & \left. - \langle \sigma_{N\phi \rightarrow \chi\nu} |v| \rangle (n_N n_\phi - \bar{n}_N \bar{n}_\phi \frac{n_\chi}{\bar{n}_\chi}) + \langle \sigma_{N\chi \rightarrow \phi\nu} |v| \rangle (n_N n_\chi - \bar{n}_N \bar{n}_\chi \frac{n_\phi}{\bar{n}_\phi}) \right\} \end{aligned}$$

$$+ \langle \sigma_{\phi\chi \rightarrow N\nu} | v \rangle (n_\phi n_\chi - \bar{n}_\phi \bar{n}_\chi \frac{n_N}{\bar{n}_N}) \Big\} , \quad (21)$$

where H is the Hubble parameter. We have made approximations given by

$$\langle \sigma_{\phi\phi \rightarrow XX'} | v \rangle = \langle \sigma_{\phi_I \phi_I \rightarrow XX'} | v \rangle \frac{\bar{n}_{\phi_I}^2}{\bar{n}_\phi^2} + \langle \sigma_{\phi_R \phi_R \rightarrow XX'} | v \rangle \frac{\bar{n}_{\phi_R}^2}{\bar{n}_\phi^2} , \quad (22)$$

$$\langle \sigma_{\phi\phi \rightarrow \chi\chi} | v \rangle = \langle \sigma_{\phi_I \phi_I \rightarrow \chi\chi} | v \rangle \frac{\bar{n}_{\phi_I}^2}{\bar{n}_\phi^2} + \langle \sigma_{\phi_R \phi_R \rightarrow \chi\chi} | v \rangle \frac{\bar{n}_{\phi_R}^2}{\bar{n}_\phi^2} , \quad (23)$$

$$\langle \sigma_{N\phi \rightarrow \chi\nu} | v \rangle = \langle \sigma_{N\phi_I \rightarrow \chi\nu} | v \rangle \frac{\bar{n}_{\phi_I}}{\bar{n}_\phi} + \langle \sigma_{N\phi_R \rightarrow \chi\nu} | v \rangle \frac{\bar{n}_{\phi_R}}{\bar{n}_\phi} , \quad (24)$$

$$\langle \sigma_{N\chi \rightarrow \phi\nu} | v \rangle = \langle \sigma_{N\chi \rightarrow \phi_I\nu} | v \rangle + \langle \sigma_{N\chi \rightarrow \phi_R\nu} | v \rangle , \quad (25)$$

$$\langle \sigma_{\phi\chi \rightarrow N\nu} | v \rangle = \langle \sigma_{\phi_R\chi \rightarrow N\nu} | v \rangle \frac{\bar{n}_{\phi_R}}{\bar{n}_\phi} + \langle \sigma_{\phi_I\chi \rightarrow N\nu} | v \rangle \frac{\bar{n}_{\phi_I}}{\bar{n}_\phi} . \quad (26)$$

As usual we rewrite (19), (20) and (21) for $Y_i \equiv n_i/s$, where s is the entropy density. To this end, we introduce the reaction rates

$$\Gamma_{ii \rightarrow XX'} = \langle \sigma_{ii \rightarrow XX'} | v \rangle \bar{n}_i , \quad (27)$$

$$\Gamma_{jj \rightarrow kk}^{(i)} = \langle \sigma_{jj \rightarrow kk} | v \rangle \frac{\bar{n}_j^2}{\bar{n}_i} \quad (\text{for } i = j \text{ or } k, m_j > m_k) , \quad (28)$$

$$\Gamma_{jk \rightarrow lX}^{(i)} = \langle \sigma_{jk \rightarrow lX} | v \rangle \frac{\bar{n}_j \bar{n}_k}{\bar{n}_i} \quad (\text{for } i = j, k \text{ or } l) . \quad (29)$$

For $i = j = \phi$, $k = \chi$, for instance, the DM conversion rate is $\Gamma_{\phi\phi \rightarrow \chi\chi}^{(\phi)}$, while is $\Gamma_{\phi\phi \rightarrow \chi\chi}^{(\chi)}$ for $i = k = \chi$, $j = \phi$. The ratio between $\Gamma_{\phi\phi \rightarrow \chi\chi}^{(\chi)}$ and $\Gamma_{\phi\phi \rightarrow \chi\chi}^{(\phi)}$ is given by the factor $\bar{n}_\phi/\bar{n}_\chi$, which is small because $m_\phi > m_\chi$. Similarly, the ratio of the semi-annihilation process and the standard annihilation for the DM i is proportional to $\bar{n}_j \bar{n}_k / \bar{n}_i^2 \sim \exp(-(m_j + m_k - 2m_i)/T) = \exp(\pm(m_j - m_k)/T)$ for $i = j$ or k . If the $\langle \sigma | v \rangle$'s are the same order of magnitude, this factor implies a larger rate in the Boltzmann equations for the heavier DM and a smaller rate for lighter DM. In the case $i = l$, the factor is $\bar{n}_j \bar{n}_k / \bar{n}_i^2 \sim \exp(-(m_j + m_k - 2m_l)/T)$ and it can be enhanced when $(m_j + m_k)/2 < m_l$. Using these reaction rates we find

$$\begin{aligned} \frac{x}{Y_N} \frac{dY_N}{dx} = & - \frac{\Gamma_{NN \rightarrow XX'}}{H(x)} \left(\frac{Y_N^2}{Y_N^2} - 1 \right) - \frac{\Gamma_{N\phi \rightarrow \chi\nu}^{(N)}}{H(x)} \left(\frac{Y_N Y_\phi}{Y_N Y_\phi} - \frac{Y_\chi}{Y_\chi} \right) \\ & - \frac{\Gamma_{N\chi \rightarrow \phi\nu}^{(N)}}{H(x)} \left(\frac{Y_N Y_\chi}{Y_N Y_\chi} - \frac{Y_\phi}{Y_\phi} \right) + \frac{\Gamma_{\phi\chi \rightarrow N\nu}^{(N)}}{H(x)} \left(\frac{Y_\phi Y_\chi}{Y_\phi Y_\chi} - \frac{Y_N}{Y_N} \right) , \end{aligned} \quad (30)$$

$$\begin{aligned} \frac{x}{Y_\phi} \frac{dY_\phi}{dx} = & - \frac{\Gamma_{\phi\phi \rightarrow XX'}}{H(x)} \left(\frac{Y_\phi^2}{Y_\phi^2} - 1 \right) - \frac{\Gamma_{\phi\phi \rightarrow \chi\chi}^{(\phi)}}{H(x)} \left(\frac{Y_\phi^2}{Y_\phi^2} - \frac{Y_\chi^2}{Y_\chi^2} \right) - \frac{\Gamma_{N\phi \rightarrow \chi\nu}^{(\phi)}}{H(x)} \left(\frac{Y_N Y_\phi}{Y_N Y_\phi} - \frac{Y_\chi}{Y_\chi} \right) \\ & + \frac{\Gamma_{N\chi \rightarrow \phi\nu}^{(\phi)}}{H(x)} \left(\frac{Y_N Y_\chi}{Y_N Y_\chi} - \frac{Y_\phi}{Y_\phi} \right) - \frac{\Gamma_{\phi\chi \rightarrow N\nu}^{(\phi)}}{H(x)} \left(\frac{Y_\phi Y_\chi}{Y_\phi Y_\chi} - \frac{Y_N}{Y_N} \right) , \end{aligned} \quad (31)$$

$$\begin{aligned} \frac{x}{Y_\chi} \frac{dY_\chi}{dx} = & - \frac{\Gamma_{\chi\chi \rightarrow XX'}}{H(x)} \left(\frac{Y_\chi^2}{Y_\chi^2} - 1 \right) + \frac{\Gamma_{\phi\phi \rightarrow \chi\chi}^{(\chi)}}{H(x)} \left(\frac{Y_\phi^2}{Y_\phi^2} - \frac{Y_\chi^2}{Y_\chi^2} \right) + \frac{\Gamma_{N\phi \rightarrow \chi\nu}^{(\chi)}}{H(x)} \left(\frac{Y_N Y_\phi}{Y_N Y_\phi} - \frac{Y_\chi}{Y_\chi} \right) \\ & - \frac{\Gamma_{N\chi \rightarrow \phi\nu}^{(\chi)}}{H(x)} \left(\frac{Y_N Y_\chi}{Y_N Y_\chi} - \frac{Y_\phi}{Y_\phi} \right) - \frac{\Gamma_{\phi\chi \rightarrow N\nu}^{(\chi)}}{H(x)} \left(\frac{Y_\phi Y_\chi}{Y_\phi Y_\chi} - \frac{Y_N}{Y_N} \right) , \end{aligned} \quad (32)$$

where $x = \mu/T$, $\mu = (M_1 + m_{\phi_R} + m_\chi)/3$, $H(x) = 1.67 g_*^{1/2} \mu^2 / m_{pl} x^2$ and g_* is the effective degrees of freedom of the massless particle in the Universe.

TABLE II. Parameter set for the calculation of Fig.6.

| M_1 | M_2, M_3 | m_{η^+} | $m_{\eta_R^0}$ | m_{ϕ_I} | m_{ϕ_R} | γ | κ | Y^ν |
|---------|------------|-------------------------|--------------------------------|-------------------|-------------------|----------|----------|---------|
| 300 GeV | 1 TeV | $m_{\eta_R^0} - 10$ GeV | $m_\chi + m_{\phi_R} - 10$ GeV | $m_\chi + 60$ GeV | $m_\chi + 50$ GeV | 0.1 | 0.4 | 0.01 |

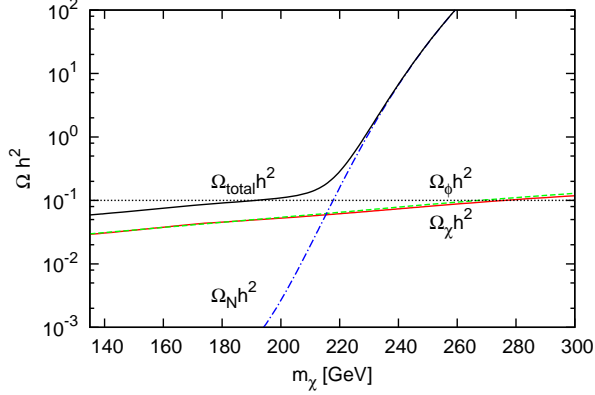


FIG. 6. The m_χ dependence of the relic density $\Omega_\chi h^2$ (red solid line), $\Omega_\phi h^2$ (green dashed line), $\Omega_N h^2$ (blue dot-dashed line) and $\Omega_{\text{total}} h^2$ (black solid line). The fixed parameters are shown in Table II.

In the original Ma model [3], the relic density of N tends to be larger than the observational value [27]. The additional contributions coming from the semi-annihilation can enhance the annihilation rate for N so that the N DM contribution to Ωh^2 can be suppressed. In this way the tension between the constraint from lepton flavor violation and the cosmological observation of Ωh^2 may become mild in the present model.

There are many mass parameters in the model, on which the relic abundance of DM depends. As a benchmark run, we vary m_χ from 135 GeV to 300 GeV with the fixed right-handed neutrino masses $M_1 = 300$ GeV and $M_2 = M_3 = 1$ TeV, while the other masses are varied with a fixed mass difference relative to m_χ i.e. $m_{\eta_R^0} = m_\chi + m_{\phi_R} - 10$ GeV, $m_{\phi_I} = m_{\phi_R} + 10$ GeV, and $m_{\phi_R} = m_\chi + 50$ GeV. Moreover, for simplicity, we use the common size of the scalar couplings, i.e. $\gamma \equiv \gamma_2 = \gamma_5 = \gamma_7$. The mass differences are chosen so that no resonance appears in the s-channel of the semi-annihilation, i.e. $m_{\eta_{R,I}^0} < m_{\phi_{R,I}} + m_\chi$. Fig. 6 shows the m_χ dependence of the individual relic densities for $\gamma = 0.1$, where the input parameters are summarized in Table II. When the scalar particles involved in the semi-annihilation are lighter than N , the semi-annihilation tends to decrease the relic density of the N DM (blue, dashed line). The total relic density of DM can be made consistent with the observed value $\Omega h^2 \sim 0.12$ [28, 29] by varying the size of the scalar couplings. Fig. 7 is a contour plot for the m_χ - γ plane. The scalar coupling γ that is consistent with $\Omega h^2 \sim 0.12$ increases drastically at $m_\chi \sim 220$ GeV because the relic density of the N DM $\Omega_N h^2$ becomes close to 0.12 at $m_\chi \sim 220$ GeV (as one can see from Fig. 6), so that $\Omega_\phi h^2$ and $\Omega_\chi h^2$ should be drastically suppressed.

A. Direct detection

The current upper bound for the DM-nucleon cross section is estimated assuming the one-component DM scenario and current upper bound and future sensitivity are given in Refs. [30–32]. Because the collision rate

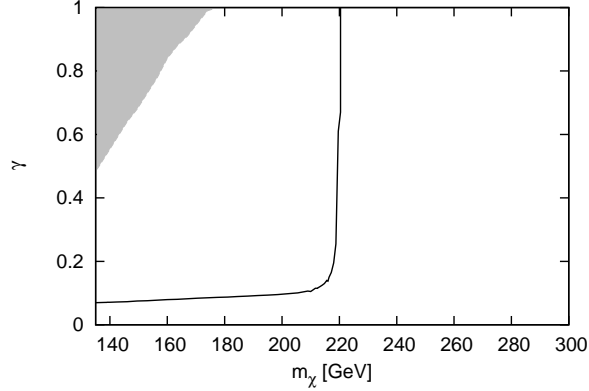


FIG. 7. Contour plot for the total relic density $\Omega_{\text{total}} h^2 \sim 0.12$. The gray region is excluded by the constraint of vacuum stability. The threshold value of m_χ depends in particular on M_1 . For the parameters given in Table II, except for $M_1 = 500$ GeV, we find $m_\chi \sim 380$ GeV, for instance.

is roughly proportional to σn_{DM} , the upper bound for the event rate can be translated to the constraint on the detection rate in the multicomponent DM scenario. The effective cross section of the nucleon corresponding to the cross section of the nucleon in the one-component DM scenario is given by

$$\sigma_i^{\text{eff}} = \sigma_i \left(\frac{\Omega_i h^2}{\Omega_{\text{total}} h^2} \right). \quad (33)$$

In our model, only ϕ_R and χ DM scatter with the nucleus, and the right-handed neutrino DM N does not interact with nucleus at tree level. So we can neglect the N contribution at the lowest order in perturbation theory. The cross sections of ϕ_R and χ are given by [11]

$$\sigma_{\phi_R} = \frac{1}{\pi} \left(\frac{(\gamma_5/2) \hat{f} m_N}{m_{\phi_R} m_h} \right)^2 \left(\frac{m_N m_{\phi_R}}{m_N + m_{\phi_R}} \right)^2, \quad (34)$$

$$\sigma_\chi = \frac{1}{\pi} \left(\frac{\gamma_2 \hat{f} m_N}{m_\chi m_h} \right)^2 \left(\frac{m_N m_\chi}{m_N + m_\chi} \right)^2, \quad (35)$$

where $\hat{f} \sim 0.3$ is the usual nucleonic matrix element [33], and m_N is the nucleon mass. Fig. 8 shows the relation between m_χ and the sum of the effective cross sections given in (33). The black line corresponds to the parameter space (the black line in Fig. 7) consistent with the cosmological observation of the DM relic abundance. Although as we see from Fig. 7, the scalar coupling γ has to become large at $m_\chi \sim 220$ GeV, such that the cross sections off the nucleon, σ_χ and σ_{ϕ_R} , become large, $\sigma_{\phi_R}^{\text{eff}} + \sigma_\chi^{\text{eff}}$ does not change very much at $m_\chi \sim 220$ GeV, because Ω_{ϕ_R} and Ω_χ both become small. We also show the result for $M_1 = 500$ GeV (the red line) in Fig. 8, where the other parameters are taken as the same as in the case with $M_1 = 300$ GeV.

B. Indirect detection

For indirect detections of DM the SM particles produced by the annihilation of DM are searched. Because the semi-annihilation produces a SM particle, this process can serve for an indirect detection. In our model, especially,

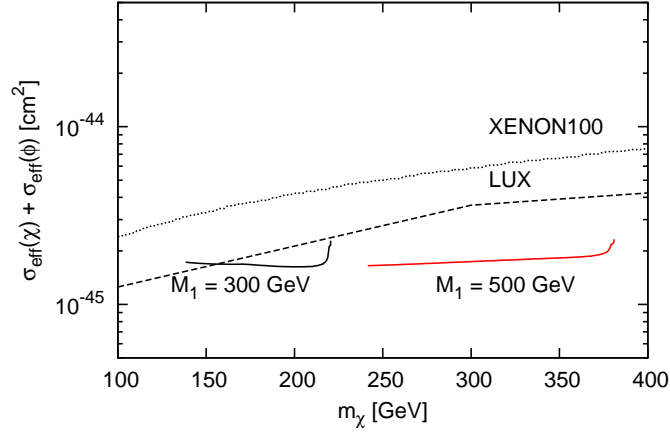


FIG. 8. The relation between the χ DM mass m_χ and the sum of the effective cross sections given in (33). The black (red) line shows the result for $M_1 = 300$ (500) GeV. The black dotted and dashed lines show the upper limit of the spin independent cross section off the nucleon given by XENON100 [30] and LUX [32], respectively.

the SM particle from the semi-annihilation process as shown in Fig. 4 is neutrino which has a monochromatic energy spectrum [10]. Therefore, we consider below the neutrino flux from the Sun [34–41] as a possibility to detect the semi-annihilation process of DMs.

The DM particles are captured in the Sun losing their kinematic energy through scattering with the nucleus. Then captured DM particles annihilate each other. The time dependence of the number of DM n_i in the Sun is given by

$$\dot{n}_i = C_i - C_A(ii \rightarrow \text{SM})n_i^2 - \sum_{m_i > m_j} C_A(ii \rightarrow jj)n_i^2 - C_A(ij \rightarrow k\nu)n_i n_j, \quad (36)$$

where C_i is the capture rate in the Sun, and C_A 's are the annihilation rates in the Sun[38, 40, 41]:

$$C_\chi \sim 1.4 \times 10^{20} f(m_\chi) \left(\frac{\hat{f}}{0.3} \right)^2 \left(\frac{\gamma_2}{0.1} \right)^2 \left(\frac{200 \text{ GeV}}{m_\chi} \right)^2 \left(\frac{\Omega_\chi h^2}{\Omega_{\text{total}}} \right)^2, \quad (37)$$

$$C_{\phi_R} \sim 1.4 \times 10^{20} f(m_{\phi_R}) \left(\frac{\hat{f}}{0.3} \right)^2 \left(\frac{\gamma_5}{0.2} \right)^2 \left(\frac{200 \text{ GeV}}{m_{\phi_R}} \right)^2 \left(\frac{\Omega_{\phi_R} h^2}{\Omega_{\text{total}}} \right)^2, \quad (38)$$

$$C_N = 0, \quad (39)$$

$$C_A(ij \rightarrow \bullet) = \frac{\langle \sigma(ij \rightarrow \bullet) | v | \rangle}{V_{ij}}, \quad V_{ij} = 5.7 \times 10^{27} \left(\frac{100 \text{ GeV}}{\mu_{ij}} \right)^{3/2} \text{ cm}^3. \quad (40)$$

Here $f(m_i)$ depends on the form factor of the nucleus, elemental abundance, kinematic suppression of the capture rate, etc., varying $\mathcal{O}(0.01 - 1)$ depending on the DM mass [40, 41]. V_{ij} is an effective volume of the Sun with $\mu_{ij} = 2m_i m_j / (m_i + m_j)$ in the nonrelativistic limit. We neglect the DM production processes in Eq.(36) like $jj \rightarrow ii$ and $jk \rightarrow iX$ because the kinetic energy of the produced particle i is much larger than that corresponding to the escape velocity from the Sun, i.e. $\sim 10^3$ km/s [38, 42]. Consequently, the number of the right-hand neutrino DM cannot increase, and hence $\phi\chi \rightarrow N\nu$ is the only neutrino production process, where its reaction rate is given by $\Gamma(\nu) = C_A(\phi\chi \rightarrow N\nu)n_\phi n_\chi$ ⁴.

⁴ There are also neutrinos having a continuous energy spectrum from the decay of standard model particles, W^+ or b for instance,

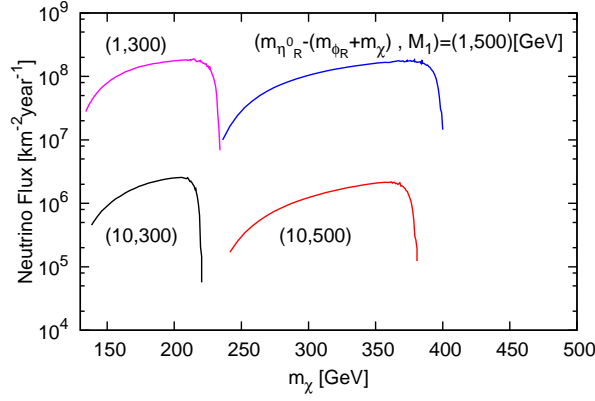


FIG. 9. The neutrino flux from the Sun on the Earth against the χ DM mass. The flux is calculated from the reaction rate $\Gamma(\nu) = C_A(\phi\chi \rightarrow N\nu)n_\phi n_\chi$, where the numbers n_ϕ and n_χ are obtained by solving the evolution equation (36) numerically. We have used four different values of $m_{\eta_R^0} - (m_{\phi_R} + m_\chi)$ and M_1 : $(m_{\eta_R^0} - (m_{\phi_R} + m_\chi), M_1) = (10 \text{ GeV}, 300 \text{ GeV})$ (black curve), $(1 \text{ GeV}, 300 \text{ GeV})$ (magenta curve), $(10 \text{ GeV}, 500 \text{ GeV})$ (red curve), and $(1 \text{ GeV}, 500 \text{ GeV})$ (blue curve), respectively.

The monochromatic neutrino flux on the Earth is roughly given by $\Gamma_{inc} = \Gamma/4\pi R_\odot^2$, where R_\odot stands for the distance to the Sun. Fig. 9 shows the m_χ dependence of the neutrino flux for the same parameter space (black line) as in Fig. 6. As we can see from Fig. 4 a resonance effect for the s-channel annihilation process can be achieved if $m_{\eta_R^0} \simeq m_{\phi_R} + m_\chi$. Obviously, the smaller the mass difference $m_{\eta_R^0} - (m_{\phi_R} + m_\chi)$ is, the larger is the semi-annihilation cross section and hence the neutrino flux. In Fig. 9 four different values are used: $(m_{\eta_R^0} - (m_{\phi_R} + m_\chi), M_1) = (10 \text{ GeV}, 300 \text{ GeV})$ (black curve), $(1 \text{ GeV}, 300 \text{ GeV})$ (magenta curve), $(10 \text{ GeV}, 500 \text{ GeV})$ (red curve), and $(1 \text{ GeV}, 500 \text{ GeV})$ (blue curve), respectively. In the case that Ω_N dominates (so that Ω_ϕ and Ω_χ are small) the capture rates of the ϕ and χ DMs become small (see (36)). This is why the neutrino flux decreases after a certain value of m_χ .

The upper limits on the defused neutrino flux from the Sun are given by the IceCube experiment [44]. The upper limit on the neutrino flux produced by the annihilation of the DMs of 250 GeV into W^+W^- , for instance, is $9.72 \times 10^{10} \text{ km}^{-2} \text{ y}^{-1}$ [44]. We can see from Fig. 9 that, unfortunately, this limit is at least 10^3 times larger than the monochromatic neutrino flux produced by the semi-annihilation of the ϕ and χ DMs. Note however, that the energy spectrum of the neutrino flux produced by the W decay is different from the monochromatic neutrino. With an increasing resolution of energy and angle the chance for the observation of the semi-annihilation and hence of a multicomponent nature of DM can increase.

IV. CONCLUSION

In this paper our interest has been directed at an indirect observation of multicomponent DM systems through semi-annihilation processes of DMs, because these processes are characteristic of multicomponent DM systems. In one-component DM systems of a real scalar boson or of a Majorana fermion the monochromatic neutrino produc-

produced by standard annihilation of scalar DMs. The upper bounds for the production rates of the standard model particles are given in [42–44].

tion by DM annihilation is due to the chirality of the left-handed neutrino strongly suppressed. The suppression due to the chirality is absent when DM is a complex scalar boson or a Dirac fermion. In a multicomponent DM system, too, the neutrino production is unsuppressed if it is an allowed process.

In this paper, instead of performing a model independent investigation on multicomponent DM systems we have first motivated the existence of a multicomponent DM system by extending the one-loop radiative seesaw model of Ma [3] to remove its shortcomings. In the model of Ma [3], the lepton-number violating mass term of the inert scalar doublet has to be very small to obtain small neutrino masses. This mass term originates from a lepton-number violating quartic scalar coupling, the " λ_5 coupling", which is $\mathcal{O}(10^{-5})$ to obtain small neutrino masses for $Y^\nu \sim 0.01$. We therefore have considered an extension of the model such that this lepton-number violating mass, too, is radiatively generated. Consequently, the seesaw mechanism occurs at the two-loop level in the extended model [4]. For this mechanism to work, we have introduced a larger unbroken discrete symmetry, $Z_2 \times Z_2$, which implies that the model yields a multicomponent DM system. We emphasize that the multicomponent DM system is a consequence of the unbroken $Z_2 \times Z_2$, which forbids the Dirac neutrino mass.

The DM annihilation processes can be classified to three types; standard annihilation, DM conversion and semi-annihilation. We have assumed that the right-handed neutrino N and two real bosons, χ and ϕ , are DM particles, and solved numerically the set of coupled Boltzmann equations. It has turned out that the semi-annihilation effect for the heaviest dark matter is considerably enhanced by the Boltzmann factor.

We have computed the spin-independent cross section of the dark matter particles ϕ and χ off the nucleon. (At the tree level there is no interaction of N with the quarks.) The quantity, which should be compared with the experimental limits, is $\sigma_{\text{eff}} = (\sigma_\chi \Omega_\chi + \sigma_\phi \Omega_\phi) / \Omega_{\text{total}}$. The predicted values of σ_{eff} have turned out to be slightly below the present limit given by LUX [32] for $m_\chi \gtrsim 150$ GeV. Since the sensitivity of XENON1T [31] will be 2 orders of magnitude higher than that of XENON100, the predicted area will be covered by XENON1T. It should, however, be emphasized that the XENON1T experiment alone cannot decide how many dark matter particles are present. A clever choice of kinematical cuts at collider experiments could be used to explore a multi-component nature of DM [45].

As mentioned above, the monochromatic neutrino production by the semi-annihilation processes $\chi N \rightarrow \nu_L \phi$, etc., is not suppressed. The time evolution of the number of the dark matter particles n_i ($i = N, \phi, \chi$) in the Sun has been studied numerically to estimate their values at the present time, where we have set the capture rate for N equal to zero. Then we have calculated the reaction rate $\Gamma(\nu)$ in the Sun, from which we have estimated the monochromatic neutrino flux coming from the Sun on the Earth and hence the monochromatic neutrino flux at the IceCube detector. It turns out that the flux is very small compared with the current IceCube sensitivity. However, the s-channel process of the semi-annihilation can be enhanced by a resonant effect: The enhanced signal is still 3 orders of magnitude smaller than the current IceCube sensitivity. Nevertheless, the higher the resolution of energy and angle is, the larger is the chance for the observation of the monochromatic neutrino and hence of a multicomponent nature of DM.

The work of M. A. is supported in part by the Grant-in-Aid for Scientific Research (Grant No. 25400250 and No. 26105509), J. K. is partially supported by the Grant-in-Aid for Scientific Research (C) from the Japan Society for Promotion of Science (Grant No. 22540271), and H. T. is supported by Japan Society for the Promotion of

-
- [1] P. Minkowski, Phys. Lett. B **67** (1977) 421; M. Gell-Mann, P. Ramond, and R. Slansky, in *Supergravity*, eds. P. van Nieuwenhuizen and D. Z. Freedman (North-Holland, 1979), p. 315; T. Yanagida, in *Proc. of the Workshop on the Unified Theory and the Baryon Number in the Universe*, eds. O. Sawada and A. Sugamoto, KEK Report No. 79-18 (Tsukuba, Japan, 1979), p. 95; R. N. Mohapatra and G. Senjanovic, Phys. Rev. Lett. **44** (1980) 912.
- [2] L. M. Krauss, S. Nasri and M. Trodden, Phys. Rev. D **67** (2003) 085002 [hep-ph/0210389]; M. Aoki, S. Kanemura and O. Seto, Phys. Rev. Lett. **102** (2009) 051805 [arXiv:0807.0361 [hep-ph]].
- [3] E. Ma, Phys. Rev. D **73** (2006) 077301 [hep-ph/0601225].
- [4] M. Aoki, J. Kubo and H. Takano, Phys. Rev. D **87** (2013) 116001 [arXiv:1302.3936 [hep-ph]].
- [5] E. Ma and U. Sarkar, Phys. Lett. B **653** (2007) 288 [arXiv:0705.0074 [hep-ph]].
- [6] Z. G. Berezhiani and M. Y. .Khlopov, Sov. J. Nucl. Phys. **52** (1990) 60 [Yad. Fiz. **52** (1990) 96]; Z. G. Berezhiani and M. Y. .Khlopov, Z. Phys. C **49** (1991) 73; T. Hur, H. S. Lee and S. Nasri, Phys. Rev. D **77**, 015008 (2008) [arXiv:0710.2653 [hep-ph]]; K. M. Zurek, Phys. Rev. **D79** (2009) 115002 [arXiv:0811.4429 [hep-ph]]; B. Batell, Phys. Rev. D **83** (2011) 035006 [arXiv:1007.0045 [hep-ph]]; K. R. Dienes and B. Thomas, Phys. Rev. D **85** (2012) 083523 [arXiv:1106.4546 [hep-ph]]; K. R. Dienes and B. Thomas, Phys. Rev. D **85** (2012) 083524 [arXiv:1107.0721 [hep-ph]]; K. R. Dienes, S. Su and B. Thomas, Phys. Rev. D **86** (2012) 054008 [arXiv:1204.4183 [hep-ph]]; D. Chialva, P. S. B. Dev and A. Mazumdar, Phys. Rev. D **87** (2013) 6, 063522 [arXiv:1211.0250 [hep-ph]]; P. -H. Gu, Phys. Dark Univ. **2** (2013) 35 [arXiv:1301.4368 [hep-ph]]; Y. Kajiyama, H. Okada and T. Toma, Phys. Rev. D **88** (2013) 1, 015029 [arXiv:1303.7356]; S. Bhattacharya, A. Drozd, B. Grzadkowski and J. Wudka, JHEP **1310** (2013) 158 [arXiv:1309.2986 [hep-ph]]; Y. Kajiyama, H. Okada and T. Toma, Eur. Phys. J. C **74** (2014) 2722 [arXiv:1304.2680 [hep-ph]]; C. -Q. Geng, D. Huang and L. -H. Tsai, Phys. Rev. D **89** (2014) 055021 [arXiv:1312.0366 [hep-ph]]; C. -Q. Geng, D. Huang and L. -H. Tsai, arXiv:1405.7759 [hep-ph].
- [7] F. D’Eramo and J. Thaler, JHEP **1006** (2010) 109 [arXiv:1003.5912 [hep-ph]]; G. Belanger, K. Kannike, A. Pukhov and M. Raidal, JCAP **1204** (2012) 010 [arXiv:1202.2962 [hep-ph]]; I. P. Ivanov and V. Keus, Phys. Rev. D **86**, 016004 (2012) [arXiv:1203.3426 [hep-ph]].
- [8] F. D’Eramo, M. McCullough and J. Thaler, JCAP **1304** (2013) 030 [arXiv:1210.7817 [hep-ph]].
- [9] E. Ma, Annales Fond. Broglie **31** (2006) 285 [arXiv:hep-ph/0607142]; E. Ma, Mod. Phys. Lett. **A23** (2008) 721 [arXiv:0801.2545 [hep-ph]]; H. Fukuoka, J. Kubo and D. Suematsu, Phys. Lett. B **678** (2009) 401 [arXiv:0905.2847 [hep-ph]]; H. Fukuoka, D. Suematsu and T. Toma, JCAP **1107** (2011) 001 [arXiv:1012.4007 [hep-ph]]; D. Suematsu and T. Toma, Nucl. Phys. B **847** (2011) 567 [arXiv:1011.2839 [hep-ph]]; M. Aoki, J. Kubo, T. Okawa and H. Takano, Phys. Lett. B **707** (2012) 107 [arXiv:1110.5403 [hep-ph]].
- [10] M. Aoki, M. Duerr, J. Kubo and H. Takano, Phys. Rev. D **86** (2012) 076015 [arXiv:1207.3318 [hep-ph]].
- [11] R. Barbieri, L. J. Hall and V. S. Rychkov, Phys. Rev. D **74** (2006) 015007 [arXiv:hep-ph/0603188].
- [12] L. Lopez Honorez, E. Nezri, J. F. Oliver and M. H. G. Tytgat, JCAP **0702** (2007) 028 [arXiv:hep-ph/0612275]; E. M. Dolle and S. Su, Phys. Rev. D **80** (2009) 055012 [arXiv:0906.1609 [hep-ph]]; M. Gustafsson, S. Rydbeck, L. Lopez-Honorez and E. Lundstrom, Phys. Rev. D **86**, 075019 (2012) [arXiv:1206.6316 [hep-ph]].
- [13] G. Aad *et al.* [ATLAS Collaboration], Phys. Lett. B **716** (2012) 1 [arXiv:1207.7214 [hep-ex]]; S. Chatrchyan *et al.* [CMS Collaboration], Phys. Lett. B **716** (2012) 30 [arXiv:1207.7235 [hep-ex]].
- [14] M. Ackermann *et al.* [LAT Collaboration], Phys. Rev. D **86** (2012) 022002 [arXiv:1205.2739 [astro-ph.HE]].
- [15] [ATLAS Collaboration], ATLAS-CONF-2013-014, ATLAS-COM-CONF-2013-025; [CMS Collaboration], CMS-PAS-

HIG-13-005.

- [16] M. Gustafsson [for the Fermi-LAT Collaboration], arXiv:1310.2953 [astro-ph.HE]; F. D’Eramo and J. Thaler, JHEP **1006**, 109 (2010) [arXiv:1003.5912 [hep-ph]]; G. Belanger, K. Kannike, A. Pukhov and M. Raidal, JCAP **1204** (2012) 010 [arXiv:1202.2962 [hep-ph]]; F. D’Eramo, M. McCullough and J. Thaler, JCAP **1304** (2013) 030 [arXiv:1210.7817 [hep-ph]]; G. Belanger, K. Kannike, A. Pukhov and M. Raidal, JCAP **1301** (2013) 022 [arXiv:1211.1014 [hep-ph]]; P. Ko and Y. Tang, JCAP **1405** (2014) 047 [arXiv:1402.6449 [hep-ph]]; G. Blanger, K. Kannike, A. Pukhov and M. Raidal, JCAP **1406** (2014) 021 [arXiv:1403.4960 [hep-ph]]; M. Aoki and T. Toma, arXiv:1405.5870 [hep-ph].
- [17] T. Hambye, JHEP **0901** (2009) 028 [arXiv:0811.0172 [hep-ph]]; C. Arina, T. Hambye, A. Ibarra and C. Weniger, JCAP **1003** (2010) 024 [arXiv:0912.4496 [hep-ph]]; V. V. Khoze, C. McCabe and G. Ro, arXiv:1403.4953 [hep-ph]; C. Boehm, M. J. Dolan and C. McCabe, Phys. Rev. D **90** (2014) 023531 [arXiv:1404.4977 [hep-ph]].
- [18] G. ’t Hooft, NATO Adv. Study Inst. Ser. B Phys. **59** (1980) 135.
- [19] R. Bouchand and A. Merle, JHEP **1207** (2012) 084 [arXiv:1205.0008 [hep-ph]].
- [20] T. Toma and A. Vicente, JHEP **1401**, 160 (2014) [arXiv:1312.2840, arXiv:1312.2840 [hep-ph]].
- [21] E. Ma and M. Raidal, Phys. Rev. Lett. **87** (2001) 011802 [Erratum-ibid. **87** (2001) 159901] [arXiv:hep-ph/0102255].
- [22] J. Adam *et al.* [MEG Collaboration], Phys. Rev. Lett. **110** (2013) 201801 [arXiv:1303.0754 [hep-ex]].
- [23] K. Hayasaka, arXiv:1010.3746 [hep-ex].
- [24] J. Beringer *et al.* [Particle Data Group Collaboration], Phys. Rev. D **86** (2012) 010001.
- [25] M. Ciuchini, E. Franco, S. Mishima and L. Silvestrini, JHEP **1308** (2013) 106 [arXiv:1306.4644 [hep-ph]].
- [26] K. Griest, D. Seckel, Phys. Rev. **D43** (1991) 3191-3203.
- [27] J. Kubo, E. Ma and D. Suematsu, Phys. Lett. B **642** (2006) 18 [hep-ph/0604114].
- [28] G. Hinshaw *et al.* [WMAP Collaboration], Astrophys. J. Suppl. **208**, 19 (2013) [arXiv:1212.5226 [astro-ph.CO]].
- [29] P. A. R. Ade *et al.* [Planck Collaboration], Astron. Astrophys. (2014) [arXiv:1303.5076 [astro-ph.CO]].
- [30] E. Aprile *et al.* [XENON100 Collaboration], Phys. Rev. Lett. **109** (2012) 181301 [arXiv:1207.5988 [astro-ph.CO]].
- [31] E. Aprile [XENON1T Collaboration], arXiv:1206.6288 [astro-ph.IM].
- [32] D. S. Akerib *et al.* [LUX Collaboration], Phys. Rev. Lett. **112**, 091303 (2014) [arXiv:1310.8214 [astro-ph.CO]].
- [33] J. R. Ellis, A. Ferstl and K. A. Olive, Phys. Lett. B **481** (2000) 304 [arXiv:hep-ph/0001005].
- [34] J. Silk, K. A. Olive and M. Srednicki, Phys. Rev. Lett. **55** (1985) 257.
- [35] L. M. Krauss, M. Srednicki and F. Wilczek, Phys. Rev. D **33** (1986) 2079.
- [36] K. Freese, Phys. Lett. B **167** (1986) 295.
- [37] T. K. Gaisser, G. Steigman and S. Tilav, Phys. Rev. D **34** (1986) 2206.
- [38] K. Griest and D. Seckel, Nucl. Phys. B **283** (1987) 681 [Erratum-ibid. B **296** (1988) 1034].
- [39] S. Ritz and D. Seckel, Nucl. Phys. B **304** (1988) 877.
- [40] M. Kamionkowski, Phys. Rev. D **44** (1991) 3021.
- [41] M. Kamionkowski, K. Griest, G. Jungman and B. Sadoulet, Phys. Rev. Lett. **74** (1995) 5174 [arXiv:hep-ph/9412213].
- [42] P. Agrawal, E. M. Dolle and C. A. Krenke, Phys. Rev. D **79** (2009) 015015 [arXiv:0811.1798 [hep-ph]]; S. Andreas, M. H. G. Tytgat and Q. Swillens, JCAP **0904** (2009) 004 [arXiv:0901.1750 [hep-ph]].
- [43] R. Abbasi *et al.* [IceCube Collaboration], Phys. Rev. D **85** (2012) 042002 [arXiv:1112.1840 [astro-ph.HE]]; T. Tanaka *et al.* [Super-Kamiokande Collaboration], Astrophys. J. **742** (2011) 78 [arXiv:1108.3384 [astro-ph.HE]].
- [44] M. G. Aartsen *et al.* [IceCube Collaboration], Phys. Rev. Lett. **110** (2013) 131302 [arXiv:1212.4097 [astro-ph.HE]].
- [45] K. R. Dienes, S. Su and B. Thomas, arXiv:1407.2606 [hep-ph].